

# Hadro-Chemistry and Evolution of (Anti-) Baryon Densities at RHIC

Ralf Rapp

*Department of Physics and Astronomy, State University of New York, Stony Brook, NY 11794-3800, U.S.A.*

(November 4, 2018)

The consequences of hadro-chemical freezeout for the subsequent hadron gas evolution in central heavy-ion collisions at RHIC and LHC energies are discussed with special emphasis on effects due to antibaryons. Contrary to naive expectations, their individual conservation, as implied by experimental data, has significant impact on the chemical off-equilibrium composition of hadronic matter at collider energies. This may reflect on a variety of observables including source sizes and dilepton spectra.

The systematic study of hadron production in central collisions of heavy nuclei at (ultra-) relativistic energies has revealed strong evidence for a high degree of equilibration achieved in the course of these reactions. In particular, it has been shown that, over a large range of collision energies (from SIS to SPS) [1–6], the measured final state hadron abundances can be well described by essentially two parameters, the temperature  $T$  and baryon chemical potential  $\mu_B$  (which bear little sensitivity on centrality [7]). Importantly, the inferred collision-energy dependence reinforces confidence in the notion that one is actually probing different regions of the QCD phase diagram in these experiments. The analyses are in line with the naive expectation that with increasing CM-energy  $\sqrt{s}$  of the colliding nuclei, the central rapidity regions are increasingly governed by interactions between low- $x$  partons of the incoming nucleons, thus leading to a decrease in the net baryon content. This is reflected in a systematic decrease of the baryon chemical potential with  $\sqrt{s}$ , accompanied by an increase in temperature. In fact, for the top SPS energies ( $\sqrt{s} = 17$  AGeV) and for the first RHIC data at  $\sqrt{s} = 130$  AGeV, the such extracted  $(\mu, T)$  values are very close to the expected phase boundary to the Quark-Gluon Plasma (QGP). Under RHIC conditions this implies a copious production of baryon-antibaryon pairs. Whether those are solely of thermal origin, or what exactly the underlying microscopic (partonic) production mechanism is, remains a matter of debate at present. It is clear, however, that, as with any hadronic observable, the impact of the later hadronic stages has to be well understood before any firm conclusions can be drawn.

At SPS and RHIC/LHC energies the total hadron densities implied by the hadro-chemical analyses are not small, and one cannot expect the system to decouple at this point. It has been realized, however, that hadronic cross sections for elastic scattering, especially when involving intermediate resonances (*e.g.*,  $\pi\pi \leftrightarrow \rho$ ,  $\pi N \leftrightarrow \Delta$ ,  $\pi K \leftrightarrow K^*$ ), are typically much larger than those for inelastic (number-changing) reactions. The associated timescales for thermal equilibration are thus much smaller than for the chemical one. At SPS energies and above, thermal equilibrium in the expanding hadron gas can be maintained for about 10 fm/c. This is much below typical chemical relaxation times and has led to the

picture of a chemical freezeout at  $(\mu_{ch}, T_{ch})$  (as inferred from hadron ratios) with  $T_{ch} \simeq 160$ –180 MeV, followed by a thermal decoupling at significantly lower temperatures,  $T_{th} \simeq 100$ –120 MeV. The existence of this intermediate hadronic phase is well supported as it importantly figures into both hadronic [8] and electromagnetic observables [9].

An immediate consequence of this picture is that all hadron species which are not subject to strong decays, have to be effectively conserved in number subsequent to chemical freezeout. In statistical mechanics language, this can be described by the build-up of (effective) chemical potentials,  $\mu_\pi$ ,  $\mu_K$ ,  $\mu_\eta$ , etc., in the hadronic evolution towards thermal freezeout. Corresponding thermodynamic trajectories at SPS energies have been constructed [20–24]. In this context, antibaryons play a special role. Although their production from AGS to RHIC energies follows chemical-freezeout systematics, this cannot be expected a priori, since their annihilation cross section on baryons is large (*e.g.*,  $\sigma_{p\bar{p} \rightarrow n\pi} \simeq 50$  mb with an average  $n=5$ –6 at the typical thermal energies). Under SPS conditions, this issue has been resolved in ref. [25], where it is shown that the backward reaction of multipion fusion, in connection with the rather large oversaturation of the pion phase space towards thermal freezeout (entailing  $\mu_\pi^{th} \simeq 70$  MeV), is capable of approximately maintaining the chemical-freezeout number of antibaryons. On the other hand, with a  $\bar{p}/p$  ratio of 5–7% [10,11] and a final  $\pi/B$  ratio (after strong decays) of around 5, the detailed treatment of antibaryons does not exert a large influence on the bulk thermodynamics of the hadronic evolution. The main point of this note is to show that this is no longer true at RHIC energies. Based on the experimental fact that also at RHIC the chemical freezeout abundances survive the hadron gas phase, we will argue that the explicit conservation of antibaryon number significantly affects the composition (and possibly evolution) of the hadronic expansion at collider energies. In particular, we will construct an explicit isentropic trajectory in the  $\mu_B$ - $T$  plane including effective number-conservation constraints.

Before we proceed with a more quantitative assessment, let us further motivate our objective by the following estimate: RHIC data at  $\sqrt{s} = 130$  AGeV for central Au-Au collisions [12–14] imply a midrapidity density of

charged pions plus kaons of about  $dN_{ch}/dy \simeq 600$ , so that  $dN_{\pi+K}/dy \simeq 900$ . On the other hand, the total baryon number has been estimated to be  $dN_B/dy \simeq 100$  [15,16] so that  $dN_{B+\bar{B}}/dy \simeq 165$  (using  $\bar{B}/B \simeq 0.65$  [17,16]). Since a (anti-) baryon carries about twice the entropy than that of pion, it follows that the former account for at least 25% of the total entropy at midrapidity.

Along the lines of standard hadro-chemical analyses we base the following calculations for the thermodynamic state variables on an ideal hadron gas\* including a set of resonance states comprised of 37 meson and 37 baryon species (up to masses  $m_M = 1.7$  GeV and  $m_B = 2$  GeV, respectively). We will focus on conditions representative for midrapidities in central Au+Au collisions at  $\sqrt{s} = 200$  AGeV (very similar results emerge for a net-baryon free environment appropriate for LHC). For definiteness, we employ a specific entropy (*i.e.*, entropy per *net* baryon) of  $S/N_B^{net} = 250$  which, together with a chemical freezeout temperature of  $T_{ch} = 180$  MeV, results in a baryon chemical potential of  $\mu_B^{ch} = 24$  MeV. This agrees well with (moderate) extrapolations of very similar thermal model analyses [26,27] based on RHIC data at  $\sqrt{s} = 130$  AGeV. By definition, all meson-chemical potentials are zero at  $T_{ch}$ , and we also neglect (small) isospin ( $\mu_I$ ) and strangeness ( $\mu_s$ ) chemical potentials. As usual, the effective pion number, which is subject to conservation, is defined by including all strongly decaying resonances with lifetimes shorter than the duration of the interacting hadronic phase, *i.e.*,

$$N_{\pi}^{eff} = V_{FB} \sum_i N_{\pi}^{(i)} \varrho_i(T, \mu_i), \quad (1)$$

and likewise for  $K$ ,  $\eta$  and  $\eta'$ . In eq. (1),  $V_{FB}$  denotes the fireball 3-volume (which is related to the centrality of the collision but does not affect thermodynamic quantities) and  $\varrho_i$  the number density of hadron  $i$ . The effective pion-number  $N_{\pi}^{(i)}$  of a given resonance is determined by the number of pions in its decay modes including the branching ratios, *e.g.*,  $N_{\pi}^{(\rho)} = 2$ ,  $N_{\pi}^{(\Delta)} = N_{\pi}^{(K^*)} = 1$ ,  $N_{\pi}^{(N(1520))} = 0.55 * 1 + 0.45 * 2$ . The same weighting applies to the corresponding effective chemical potential of each resonance, *e.g.*,  $\mu_{\rho} = 2\mu_{\pi}$ ,  $\mu_{\Delta} = \mu_N + \mu_{\pi}$ ,  $\mu_{K^*} = \mu_{\pi} + \mu_K$ ,  $\mu_{N(1520)} = \mu_N + 1.45\mu_{\pi}$ , which means that the strong decays and formations are in relative chemical equilibrium. For a few states this distinction is not very sharp, most notably  $\omega$  and  $\phi$  mesons. Their free lifetimes are well above hadronic fireball lifetimes, but in-medium effects are expected to alter this situation [28–33]. In the former case, some of the  $\omega$ 's and  $\phi$ 's decay after chemical freezeout without being regenerated, *i.e.*, their number decreases; in the latter case,

\*for a discussion of the influence of hadronic in-medium effects, see, *e.g.*, refs. [18,19].

their abundances stay (at least for a while) in chemical equilibrium which, in the case of large pion- and kaon-chemical potentials, could even increase their numbers. In our calculation we employ an intermediate scenario keeping the individual  $\omega$  and  $\phi$  numbers approximately constant (which is numerically close to the chemical equilibrium assumption). An important point now is the treatment of antibaryons as first pointed out in ref. [33]. We also conserve their number by introducing another effective chemical potential  $\mu_B^{eff}$ ; this implies, *e.g.*,  $\mu_{\bar{N}} = -\mu_N + \mu_B^{eff}$ ,  $\mu_{\bar{\Delta}} = -\mu_N + \mu_B^{eff} + \mu_{\pi}$ .

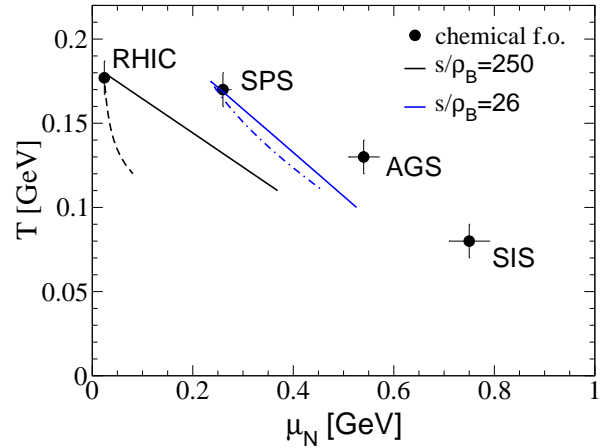


FIG. 1. Isentropic thermodynamic trajectories at RHIC (left) and SPS (right) energies, starting from the empirically determined chemical-freezeout points [1,2,5,26]. Full lines include antibaryon-number conservation, dashed lines do not. (Also note that the trajectories converge towards the zero-temperature axis at  $\mu_N = m_N$ .)

A thermodynamic trajectory in the  $\mu_N$ - $T$  plane is now constructed starting from chemical freezeout under the additional assumption of total entropy conservation (as applied in ideal fluid dynamics). Together with *net* baryon number conservation (which is, of course, exact) this amounts to keeping the specific entropy per *net* baryon fixed,  $S/N_B^{net} = s/\varrho_B^{net} = 250$  for RHIC with

$$s = \mp \sum_i d_i \int \frac{d^3k}{(2\pi)^3} [\pm f(\omega_i) \ln f(\omega_i) + (1 \mp f(\omega_i)) \ln(1 \mp f(\omega_i))], \quad (2)$$

$$\varrho_B^{net} = \sum_i d_{B_i} \int \frac{d^3k}{(2\pi)^3} [f^{B_i}(\mu_{B_i}, T) - f^{\bar{B}_i}(\mu_{\bar{B}_i}, T)] \quad (3)$$

denoting entropy- and net baryon number-density, respectively (in eq. (2), upper (lower) signs refer to fermions (bosons), and  $f$  are the pertinent thermal distribution functions). The resulting trajectory is shown by the full line in Fig. 1. For comparison, we also display a trajectory without antibaryon-number conservation (dashed line). The difference is rather dramatic,

indicating a strongly increased baryon chemical potential towards the regions of expected thermal freezeout at around  $T_{th} \simeq 120$  MeV. This is induced by an approximately linear increase of the antinucleon chemical potential, which is displayed in Fig. 2 along with nucleon, pion, kaon, and eta chemical potentials. At chemical freezeout the sum of baryon and antibaryon density is close to nuclear saturation density  $\rho_0 = 0.16 \text{ fm}^{-3}$ ,  $\varrho_{B+\bar{B}} \simeq 1.1\varrho_0$ . On the other hand, at  $T = 120$  MeV,  $\varrho_{B+\bar{B}} \simeq 0.3\varrho_0$  for the solid-line trajectory, but  $\varrho_{B+\bar{B}} \simeq 0.02\varrho_0$  for the dashed-line trajectory.

One can readily verify that the solid-line trajectory in Fig. 1 is consistent with the measured  $\bar{p}/p$  ratio, which is approximately given by  $\exp[-\Delta\mu_N/T]$  with  $\Delta\mu_N = \mu_N - \mu_{\bar{N}}$ . It is also important to note that in the  $\mu_B^{eff} \equiv 0$  case, the pion-chemical potentials remain close to zero. Thus,  $\bar{B}$  conservation at collider energies is at the origin of large meson chemical potentials in the late hadronic stages<sup>†</sup>. The reason can be traced back to the substantial amount of entropy stored in  $B\bar{B}$  excitations. At a given temperature, the smaller available entropy per pion at fixed pion number can only be realized by a finite  $\mu_\pi$ , as also noted in ref. [34]. To illustrate this fact, we display in Fig. 3 the entropy per pion in a  $\pi$ - $\rho$  gas. One finds that for  $T = 120$  MeV,  $S/N_\pi$  is reduced by about 20% when raising  $\mu_\pi$  from zero to its actual value of  $\sim 80$  MeV corresponding to the solid-line RHIC-trajectory of Fig. 2. This is in line with the rough estimate of the entropy carried by  $B\bar{B}$  pairs at RHIC above.

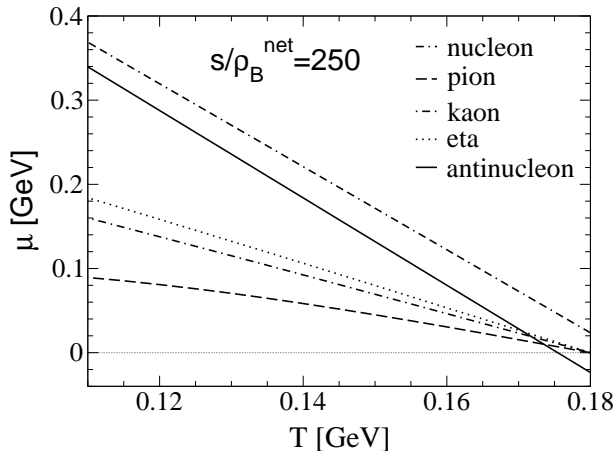


FIG. 2. Temperature dependence of nucleon-, pion-, kaon-, eta- and antinucleon-chemical potentials for an isentropic hadronic fireball expansion at RHIC energy (200 AGeV).

<sup>†</sup>This is opposite to SPS conditions, where, following the arguments of ref. [25], pion-oversaturation is responsible for regenerating antibaryons.

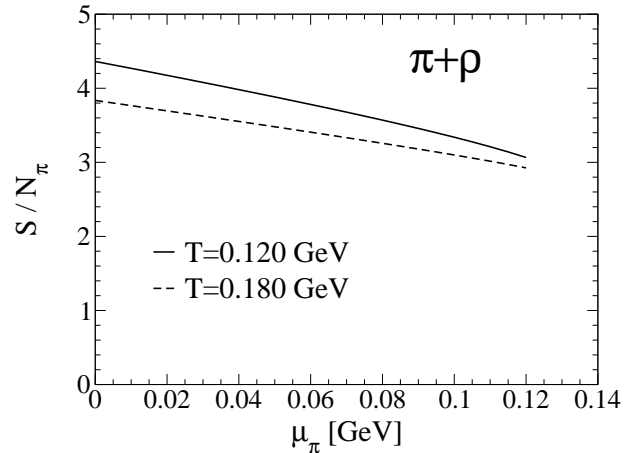


FIG. 3. Entropy per pion in a  $\pi$ - $\rho$  gas at fixed temperature as a function of pion-chemical potential (using  $\mu_\rho = 2\mu_\pi$  and counting  $\rho$ 's as two pions).

It furthermore follows that at given temperature the fireball volume  $V_{FB}$  of the system with finite  $\mu_B^{eff}$  is substantially reduced, *i.e.*, the expanding hadron gas cools faster. *E.g.*, at  $T = 120$  MeV the ratio of the 3-D fireball volumes for the  $\mu_B^{eff} \equiv 0$  and  $\mu_B^{eff} > 0$  solution for the trajectories amounts to a factor of  $\sim 3$ . Whether this will translate into smaller source size radii as extracted via HBT correlation measurement (and thus contribute to an explanation of the current 'HBT-puzzle' [35]) remains to be investigated within a (hydro-) dynamical simulation. Other observable consequences of the increased densities in the hadronic phases at RHIC concern low-mass dilepton emission, where in-medium effects are rather sensitive to (the sum of) anti-/baryon densities [9,29]. Accordingly improved estimates have been presented in ref. [33].

In our analysis we did not allude to underlying mechanisms that could provide a constant antibaryon abundance in the hadronic phase at RHIC. As mentioned above, at SPS energies this issue could be resolved [25] within a thermal framework by accounting for multi-pion fusion reactions in the presence of a large  $\mu_\pi$ . Although it is conceivable that this mechanism is also operative at RHIC, the situation is more involved due to the feedback of the  $\bar{B}$  abundance on  $\mu_\pi$ . This problem is not easily addressed within transport or cascade simulations either due to the difficulties of treating the backward reaction of multi-pion fusion (see ref. [36] for recent progress). Corresponding trajectories that have been extracted from, *e.g.*, UrQMD transport calculations [37] are therefore resembling the dashed lines in Fig. 1.

In summary, based on the notion of hydro-chemical freezeout, we have constructed (isentropic) thermodynamic trajectories for the hadronic phase in ultra-relativistic heavy-ion collisions. Consistency with the

observed particle ratios has been enforced by effective conservation laws, implemented via finite chemical potentials for stable hadrons (*w.r.t.* strong interactions). The main emphasis was on consequences of conserved antibaryon-number. At SPS energies and below, these are small, but at collider energies (RHIC and LHC) we have found appreciable modifications in the composition of the expanding hadronic system. In particular, the entropy carried by  $B\bar{B}$  pairs is not small and has been identified as the origin of large meson-chemical potentials, which in turn leads to smaller and thus denser systems at temperatures prior to thermal freezeout. This could have important consequences for hadronic and electromagnetic observables, such as source radii and medium effects in low-mass dilepton production. The former are rather sensitive to the detailed expansion dynamics of a heavy-ion reaction, which we did not address here. For the same reason, the question *where* on the given trajectories thermal freezeout in the hadronic phase occurs has not been answered, but needs to be investigated in hydrodynamical and/or microscopic transport simulations.

This work was supported by the U.S. Department of Energy under Grant No. DE-FG02-88ER40388.

- 
- [1] P. Braun-Munzinger, J. Stachel, J.P. Wessels and N. Xu, Phys. Lett. **B344** (1995) 43.
  - [2] P. Braun-Munzinger, J. Stachel, J.P. Wessels and N. Xu, Phys. Lett. **B365** (1996) 1;  
P. Braun-Munzinger, I. Heppe and J. Stachel, Phys. Lett. **B465** (1999) 15.
  - [3] G.D. Yen and M.I. Gorenstein, Phys. Rev. **C59** (1999) 2788.
  - [4] J. Rafelski and J. Letessier, hep-ph/9903018.
  - [5] J. Cleymans and K. Redlich, Phys. Rev. **C60** (2000) 054908.
  - [6] F. Becattini, J. Cleymans, A. Keränen, E. Suhonen and K. Redlich, Phys. Rev. **C64** (2001) 024901.
  - [7] J. Cleymans, B. Kämpfer and S. Wheaton, Phys. Rev. **C65** (2002) 027901.
  - [8] R. Stock, Nucl. Phys. **A661** (1999) 282.
  - [9] R. Rapp and J. Wambach, Adv. Nucl. Phys. **25** (2000) 1.
  - [10] M. Kaneta for the NA44 collaboration, Nucl. Phys. **A638** (1998) 419.
  - [11] F. Sikler for the NA49 collaboration, Nucl. Phys. **A661** (1999) 45.
  - [12] PHOBOS Collaboration (B.B. Back *et al.*), Phys. Rev. Lett. **85** (2000) 3100.
  - [13] PHENIX Collaboration (K. Adcox *et al.*), Phys. Rev. Lett. **86** (2001) 3500.
  - [14] STAR Collaboration (C. Adler *et al.*), Phys. Rev. Lett. **87** (2001) 112303.
  - [15] I. Tserruya, Proc. of ICPAQGP (Jaipur, 26.-30.12.01), to appear in PRAMANA.
  - [16] PHENIX Collaboration (K. Adcox *et al.*), nucl-ex/0112006.
  - [17] STAR Collaboration (C. Adler *et al.*), Phys. Rev. Lett. **86** (2001) 4778.
  - [18] M. Michalec, W. Florkowski and W. Broniowski, Phys. Lett. **B520** (2001) 213.
  - [19] D. Zschesche *et al.*, Nucl. Phys. **A681** (2001) 34.
  - [20] H. Bebie, P. Gerber, J.L. Goity and H. Leutwyler, Nucl. Phys. **B378** (1992) 95.
  - [21] C. Song and V. Koch, Phys. Rev. **C57** (1997) 3026.
  - [22] C.M. Hung and E. Shuryak, Phys. Rev. **C57** (1998) 1891.
  - [23] S. Pratt and K. Haglin, Phys. Rev. **C59** (1999) 3304.
  - [24] R. Rapp and J. Wambach, Eur. Phys. J. **A6** (1999) 415.
  - [25] R. Rapp and E.V. Shuryak, Phys. Rev. Lett. **86** (2001) 2980; Proc. of the Int. Workshop XXX on Gross Properties of Nuclei and Nuclear Excitations (Hirschegg, 13.-19.01.02), nucl-th/0202059.
  - [26] P. Braun-Munzinger, D. Magestro, K. Redlich and J. Stachel, Phys. Lett. **B518** (2001) 41.
  - [27] N. Xu and M. Kaneta, Nucl. Phys. **A698** (2002) 306.
  - [28] E. Oset and A. Ramos, Nucl. Phys. **A679** (2001) 616.
  - [29] R. Rapp, Phys. Rev. **C63** (2001) 054907.
  - [30] R. Schneider and W. Weise, Phys. Lett. **B515** (2001) 89.
  - [31] M. Post and U. Mosel, Nucl. Phys. **A688** (2001) 808.
  - [32] L. Alvarez-Ruso and V. Koch, nucl-th/0201011.
  - [33] R. Rapp, Proc. of the 18. Winter Workshop on Nuclear Dynamics (Nassau, Bahamas, 20.-27.01.02), to be published in Heavy Ion Phys., and nucl-th/0204003.
  - [34] J. Sollfrank and U. Heinz, Phys. Lett. **B289** (1992) 132.
  - [35] U. Heinz and P. Kolb, hep-ph/0204061.
  - [36] W. Cassing, Nucl. Phys. **A700** (2002) 618.
  - [37] L. Bravina *et al.*, Phys. Rev. **C63** (2001) 064902.